Identification of Key Mechanism Behind Arc Re-ignition in LC Commutator-Based DC Circuit Breakers

Jing Nan, George Chen, Igor O. Golosnoy
School of Electronics and Computer Science
University of Southampton
Southampton, UK
J.Nan: jn1n19@soton.ac.uk

***Abstract*—High Voltage Direct Current (HVDC) systems, crucial for renewable energy and long-distance transmission, encounter DC fault management challenges due to absent natural zero crossings and rapid fault propagation, causing energy dissipation and re-ignition issues during DC interruption. Prior research has identified various factors influencing re-ignition, including current magnitude, zero-crossing slope, and cooling efficacy. However, experimental variation in these factors often leads to contradictory outcomes, highlighting a gap in our understanding of re-ignition phenomena.**

This paper examines DC circuit breakers, particularly LC commutator-based compact breakers, efficient in rapidly commutating fault currents to a capacitor, reducing contact erosion. These breakers offer effective DC fault interruption solutions, but arc re-ignition management is a persistent challenge. The focus is on identifying critical mechanisms behind arc re-ignition. Our study presents an integrated model combining arc physics with LC circuitry to simulate arcing stages in DC interruption. Investigating three electrode cooling scenarios, we emphasize the importance of the thin boundary layer to prevent re-ignition. Two strategies are proposed to improve breaker performance: increasing sheath voltage via contact material changes or extending cooling time with a larger capacitor. These approaches highlight the vital role of boundary layer temperature management in preventing re-ignition, offering significant insights for advancing HVDC fault management.

***Index Terms*—Arc re-ignition, Plasma simulation, DC circuit breakers, LC commutation circuit**

I. Introduction

With the increasing demand for renewable energy sources and their integration into the power grid, the role of HVDC systems has become more prominent [1]. To integrate numerous large-sized generators spread across vast areas, the concept of Multi-terminal(MT) HVDC systems is proposed. Several MT HVDC projects are developing like [2] and [3]. However, their development is limited by the lack of effective DC fault management strategies. The traditional methods for DC fault protection could be divided into three categories [4]: Using the AC circuit breaker to interrupt the fault from the AC side; Employing the converter to block the fault [5], [6]; And using the DC circuit breakers to interrupt the fault from the DC side. The first approach only works for point-to-point configurations, for MT configuration which poses a challenge to disrupt the whole network [7]. Converter blocking can isolate DC faults within milliseconds, but it necessitates a greater number of switches, which can elevate costs, power losses and control intricacies [4]. Switching off the DC fault from the DC side is identified as the most cost-effective and flexible solution for DC interruption because it could clear the DC fault without causing widespread power outages [8] and has the potential to reduce the infrastructure cost by minimising the number of converters [1].

The existing solutions for circuit breakers could be divided into two main categories [8]: 1) Semiconductor-based circuit breakers, typically containing the solid-state and hybrid type. 2) Mechanical-based circuit breakers such as air circuit breakers [9], vacuum interrupters [10], and oil-based interrupters. The primary limitation of semiconductor-based circuit breakers lies in their significant conduction losses under normal working conditions and the inherent thermal constraints of electronic devices. While mechanical-based circuit breakers have issues with arcing, slow fault clearing time and electrode wear and tear due to arcing. However, recent research proposed an emerging solution: an LC commutator-based mechanical circuit breaker, which efficiently transfers DC fault current into a capacitor in just microseconds, and the device has the advantage of compact size, with simple components and lower cost [9], making it a promising option.

The LC commutator-based mechanical circuit breaker, while innovative, encounters challenges with the re-ignition phenomenon, particularly in DC systems. Unlike AC systems, where the alternating waveform of current and voltage offers multiple opportunities to diminish the arc through natural reduction of Joule heat at zero currents, steady currents in DC systems support the arc and complicate the interruption. Once the system voltage is raised by a sheath voltage, the arc will continue to burn. Therefore, understanding this transient voltage rise and its associated phenomena is crucial. Current research provides insights but also highlights limitations. For instance, a study by [9] demonstrated that their device could effectively commutate a 400A fault current, yet it failed at

a slightly higher current of 430A. Similarly, [10] reported successful interruption at 16kA, but observed re-ignitions at a much lower current of 0.5kA. These findings indicate a significant gap in our understanding of the re-ignition phenomena. Factors contributing to re-ignition are multifaceted, including the current magnitude, the slope of the current at zero crossing, and the gap distance required for voltage withstanding [4], [11]. All these complex factors require a deep understanding of arc development and decay for effective interruption. Instead of conducting a large number of experiments we use multi-physic simulations to identify the key mechanism leading to re-ignition. With a clear understanding of these physical causes, we can then devise appropriate mitigating strategies.

This paper employs multi-physics simulations to examine the arcing phenomena that occur during the interruption process of a DC circuit breaker. It explores this under three hypothetical heat transfer coefficients and delves into the behaviour of the circuit and the underlying physical phenomena. It also identifies the physical responsible for re-ignition phenomena and proposes two strategies for mitigating this issue.

II. Model Formulation

A. Thermal Plasma Model

Conventional plasma simulation methods are applied, treating the plasma as a Magnetohydrodynamic (MHD) entity, and the gas-dynamic process is governed by the conservation laws for mass, momentum and energy, these laws culminate in the well-established differential equations for fluid flow, as detailed work in [12]. For electromagnetic aspects, the simulation incorporates the electrical potential, the current density and the magnetic flux density. These electromagnetic processes are broadly governed by Maxwell's equations, a complex set of partial differential equations, as discussed by [13]. Addressing the challenge of accurately representing energy transport via radiation, our simulation employs the Net Emission Coefficient (NEC) method to approximate the emission calculations [14]. The material properties of air are adapted from [15].

B. Boundary Layer Model

Modelling the sheath-boundary layer between the arc and electrodes is complex, involving multiple sub-layers. While only the collision less sheath is considered here, it plays a crucial role in the voltage drop and electrode heating [16]. Practically, a simplified description of the entire boundary layer is necessary, utilizing interpolation based on the results of [18]. The sheath is an extremely thin layer within the boundary layer, typically micrometers thick, whereas the boundary layer itself is much larger. The sheath acts as a collisionless region where charged particles are accelerated towards the electrodes. Additionally, there are non-equilibrium layers within the boundary layer that involve collisions and non-equilibrium plasma. Modeling these layers is intricate and time-consuming, as shown in published works by [17] and [18]. To effectively connect the electrode surfaces with the equilibrium plasma, it is crucial to consider the entire boundary layer, not just the sheath. The model ignores work function reduction and electrode heating, assuming a constant ΔV=16V, which is a simplification. While ΔV affects electron breakdown, our paper focuses on thermal breakdown. This crude approximation allows us to concentrate on thermal breakdown and understand how cooling may impact it. Future work will combine both mechanisms. Currently, this approach provides an efficient way to study thermal breakdown, making it a useful approximation. The physical mechanism determining thermal breakdown is Joule heating. The sheath disappears when the current drops to zero. Our focus is on re-ignition when the current is zero, resulting in the loss of the sheath as a key element. We assume a minimum of 16V is needed to initiate an arc, based on experimental observations [9]. Regarding sheath or boundary layer modelling, whether considering electric breakdown or thermal runaway, a highly conductive gas can still exist in the boundary layer at relatively high applied voltages between contacts, allowing for electric conduction.

We assume that once the voltage exceeds 16V, the surrounding plasma becomes hot enough to heat the boundary layer sufficiently, enabling it to conduct. This is the key assumption in our model.

- Geometry: The two symmetric cylindrical geometries are referred to as the experimental device [9]. As shown in Figure 1, the air domain is a rectangle with a length of 40mm and a width of 20mm, anode and cathode are both made of copper. The geometry of electrodes is 9mm in height with a 3mm radius. The fixed gap is 2mm for simplicity.

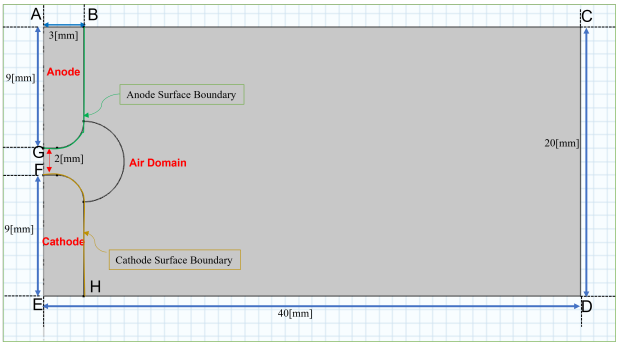

Fig. 1: Details of the computational domain of two cylindrical electrode circuit breakers

- Boundary conditions are conventional [19].
  - Electric boundary is set to AB with terminal, EH connects with the ground.
  - The external boundary temperature of electrodes is set at 300K and assigned to AB and EH. Other external boundaries as BH, CD, and DH are set as 1000K. It is artificial, but such high T was used to approximate real conditions at a short distance gap.
  - The heat transfer between the electrode and plasma domain is considered convective heat flux conveyed

by heavy particles because the main particle that affects the arc column temperature is heavy particle flux [17]. The heat flux denoted as q_0 is assigned to BG and FH.

The arc cooling is driven by the heat transfer conducted by heavy particles. And the thickness of the boundary layer is assumed to be 0.1mm in my case [18]. Hence, the heat transfer coefficient and heat flux are expressed as follows:

$$q_0 = h_{\text{heavy}} \times (T_{\text{external}} - T_{\text{plasma}}) \quad (1)$$

$$h_{\text{heavy}} = -\lambda_{\text{plasma}}(T_a) \times \frac{1}{\Delta d} \quad (2)$$

Here, $\lambda_{\text{plasma}}(T_a)$ represents the thermal conductivity of plasma, and T_{external} is the ambient temperature which is set at 300K. Note that it is assumed that the temperature of heavy particles T_a is the average temperature of plasma and electrodes.

- Heat Source and Volume Force: Joule heating and thermal radiation and thermal diffusion are implemented to the air domain. Also both the V×B as Lorentz force in the local emf and current density j×B in volume force are considered. The details formula refers to the [12], [14].

C. Modelling of Commutative DC Circuit Breaker

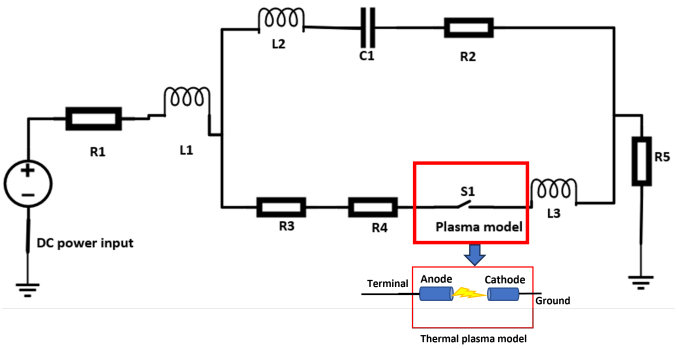

Fig. 2: Schematic of the equivalent electric circuit of circuit breaker coupled with physic arc model

The schematic in Figure 2 depicts a DC circuit breaker combined with a thermal plasma model. The DC power supply is 1000 V, and the resistor R_1 = 2.1 Ω, functions as a current limiter, while R_2, with a minimal resistance of 0.0075 Ω, represents the resistance of the transmission line. R_3=0.01 Ω represents the total resistance of the connecting wires and the electrodes. The dynamic resistor R_4 models the non-linear behaviour of the thermal plasma, with resistance varying with the current through the arc. In the proposed simplified model, R_4 is selected to supply a fixed sheath voltage drop of 16V as measured in the experiments [9]. In steady state, the short-circuit current is given by $I_{\text{sc}} \approx \frac{V_1}{R_1}$, because the resistance of R4 is much smaller than R1. I_{sc} serves as the initial condition for the circuit and is applied to the inductor L_1, valued at 10 mH. A smaller inductor L_2, at 227 nH, along with capacitor C_1, of 208 μF, create an oscillatory circuit. L_3 is used to add the model stability as the inductance of arc, which is equal to 10 nH. In the model, we start with an already open CB with voltage, we considered the typical case to refer to the parameter from [20].

Arc cooling was considered as the decay mechanism under limiting cases but using different heat transfer coefficients.

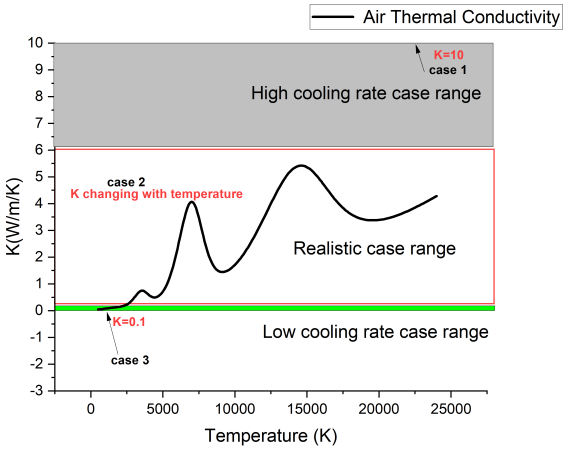

Fig. 3: Air thermal conductivity as a function of the temperature refers to three hypothetical heat transfer coefficients

- Under the assumption of a high cooling rate, thermal equilibrium is presumed at the electrode's surface. We postulate that the heat transfer coefficient, denoted as h_1, is approximately $1 \times 10^5 [\, W/m/K]$.
- According to the structure of the arc, the narrow boundary layer between the electrodes and the arc fall region is characterised by non-equilibrium conditions [18]. When current passes through the sheath layer and over the electrode surface, a certain amount of heat flux is generated. This scenario has been modelled with a 0.1 mm boundary layer, considering the average temperature of the plasma and electrodes. Consequently, it is assumed that the heat transfer coefficient, denoted as h_2, is approximately $1 \times 10^3 [W/m/K]$ as a low cooling rate assumption.
- Another realistic case is using the dynamic heat transfer coefficient donated as h_3 is equal to h_{heavy} refer to Equation 2.

For a plasma temperature potentially exceeding 25000K for a few kA currents and with a boundary layer thickness of 0.1mm, a well-cooled environment would exhibit a thermal conductivity close to 10 $[W/m/K]$. Referring to Figure 3, we can observe that the maximum thermal conductivity would be approximately 6 $[W/m/K]$, even though our assumption exceeds this number. It still qualitatively represents the concept of good cooling.

When assuming that the arc commutation process has concluded and the system reverts to a cold state, the thermal conductivity drops to around 0.1 $[W/m/K]$, correlating with a temperature of approximately 2500K. This aligns with actual

scenarios observed in practice, thereby lending practical validity to our coefficient selection and the underlying assumptions [21].

For h_3 which is dynamically changing with temperature, allows the simulation to more closely mimic or predict real outcomes.

III. Results and Discussion

A. Re-ignition Analysis

Case 1: High cooling rate $h = h_1$

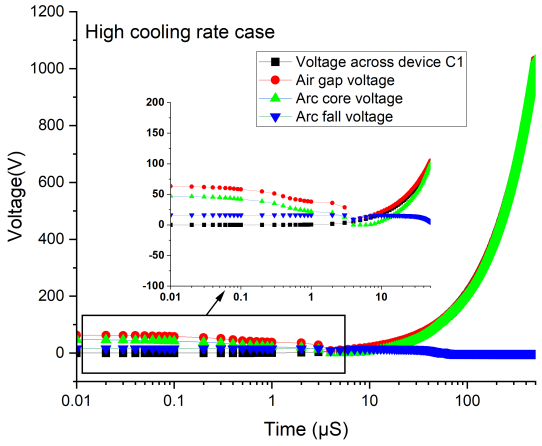

Fig. 4: Voltage profile goes through the air gap and capacitor for high cooling rate case $h = h_1$

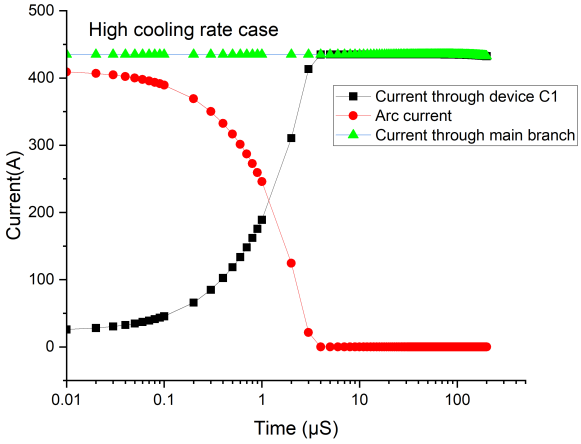

Fig. 5: Current profile goes through the air gap and capacitor for high cooling rate case $h = h_1$

- Circuit behaviours: Normally, the arc branch has lower impedance which allows the current all go through the arc branch, when we open the branch it increases the resistance of the branch, which pushes the current back to the LC commutative branch with some delay. In the model, we start with already open circuit breakers with small voltage there and it needs $3\mu s$ as settlement time, which means in a high cooling rate case the commutation process is completed within this time frame. After that, the cooling process is continuous with the equally increasing rate of voltages in both branches. The current all goes through the LC circuit with the arc extinguished.
- Physic side phenomena: An interesting phenomenon is observed following the first zero current crossings: the formation of a thin cold boundary layer as shown in Figure 6. This means the boundary layer is cooled enough to prevent the breakdown. Combined with the circuit behaviour, a successful commutation and arc interruption are observed as shown in Figure 5.

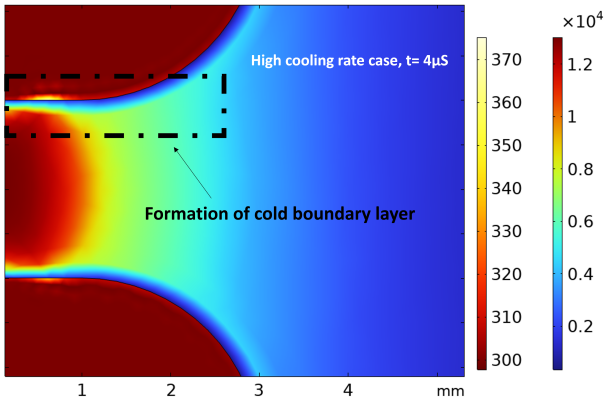

Fig. 6: Temperature distribution for high cooling rate case of boundary layer formation $h = h_1$, $t = 3\mu s$

In summary, for the high cooling rate case, the commutation could be completed within 3 microsecond. For the cold air gap, it could withstand the high breakdown voltage of nearly 1000V.

Case 2: Low cooling rate $h = h_2$

- Circuit behaviours: We start with a 2mm open air gap and trigger the commutation branch when t=0.01 μs. And commutation process is initiated, marked by a simultaneous decrease in arc current and an increase in the current of capacitor C1. The differential between these currents leads to the first current zero-crossing at around 4 μs. The circuit attempts to maintain this zero-current state, but during this holding period, the arc fall voltage across the gap increases, and so does the charge on the capacitor. At 5 μs, a re-ignition occurs when the charging the slope of the capacitor matches the increasing rate of the air gap voltage. Consequently, the voltage across the arc core becomes significant as shown in Figure 7. A critical observation during the zero-current phases is that the voltage remains relatively stable and the value is low around 16V. However, it is during these phases that the gap is prone to breakdown, potentially re-establishing current flow through the circuit.

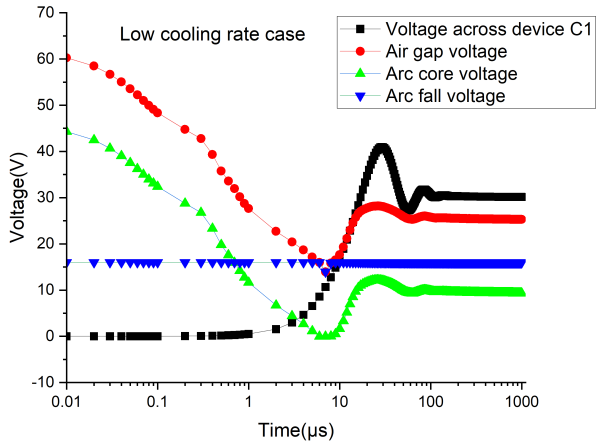

Fig. 7: Voltage profile goes through the air gap and capacitor for low cooling rate case $h = h_2$

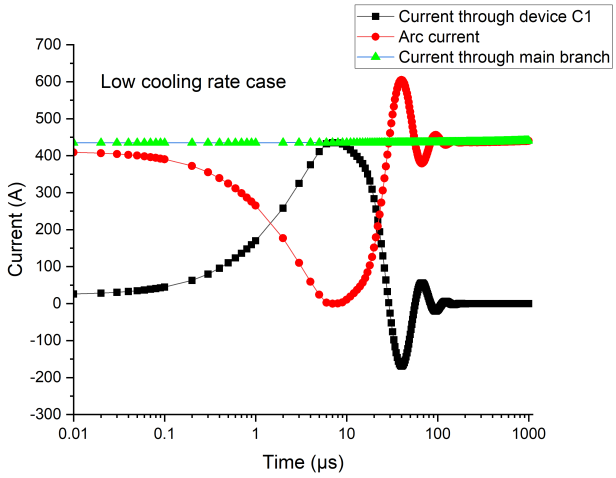

Fig. 8: Current profile goes through the air gap and capacitor for low cooling rate case $h = h_2$

- Physic side phenomena: As illustrated in Figure 9, although the circuit indicates that the current is interrupted at $3\,\mu s$, the temperature within the boundary layer remains high enough to conduct current even after $8\,\mu s$, the gap voltage rises to 16V needed to sustain the arc and arc re-ignite. Because using the LC commutative branch to extinguish the arc does not disconnect the power supply, we effectively reduced the impedance and switched off the current. If we don't limit the arc voltage, it will sustain in the arc. This elevated temperature is likely a primary factor contributing to the occurrence of a re-ignition. The key mechanism behind the re-ignition is the temperature and the conductivity of the thin boundary layer.

Case 3: Realistic cooling rate $h = h_3$ based on T_{plasma}

- Circuit behaviours: In the realistic cooling rate case

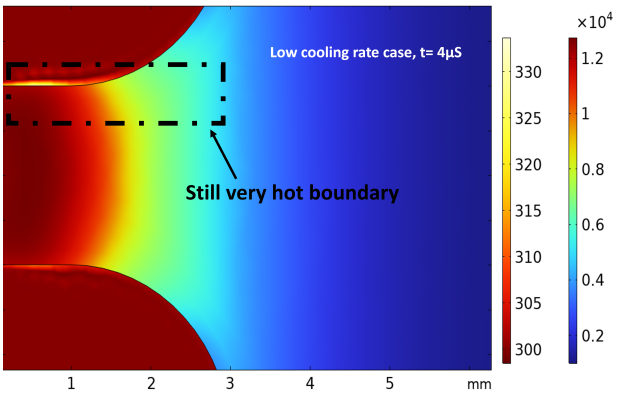

Fig. 9: Temperature distribution for low cooling rate case of boundary layer h=h_2,t=5μs

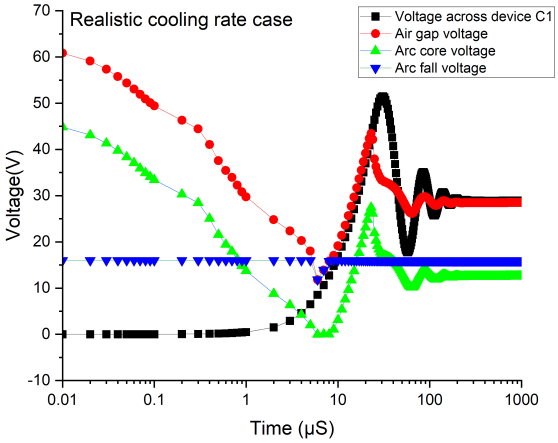

Fig. 10: Voltage profile goes through the air gap and capacitor for realistic cooling rate example $h = h_3$

scenario, the observed circuit behaviour exhibits consistent patterns as in the previous case. The commutation process takes approximately $3\,\mu s$, accompanied by an observable offset between the arc current and the current generated by the capacitor. A notable event is the first current crossing, which occurs at around $4\,\mu s$. This timing suggests an extended duration of the zero crossing period from 4 to 15 μs. Interestingly, a re-ignition phenomenon is observed at approximately $20\,\mu s$. Further examination of the voltage behaviour during the current zero period reveals that the voltage remains relatively low. However, a re-ignition still occurs despite this low voltage. This re-ignition appears to be triggered when the slope of the voltage charging the capacitor becomes equivalent to the increase in the air gap. This indicates a critical point where the conditions for re-ignition are met. Compared with the high cooling rate case the action of the circuit is the same, but the results are different.

- Physic side phenomena: Similarly, the hot boundary layer

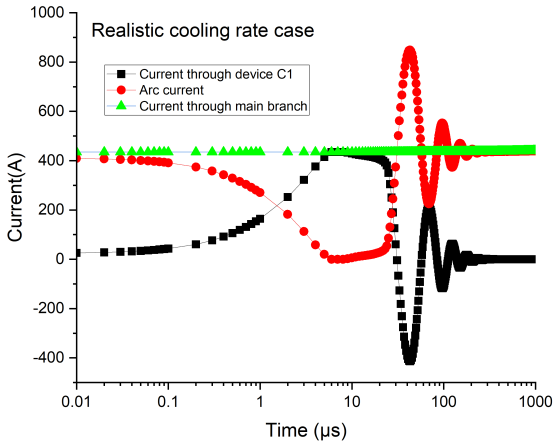

Fig. 11: Current profile goes through the air gap and capacitor for realistic cooling rate example $h = h_3$

is identified as the main cause of re-ignition as shown on the left side of Figure 14, combined with the circuit behaviour the current is stopped but the remained hot air gap allows the voltage to break through the gap.

The key distinction between the low cooling rate case and the realistic cases lies in the near-commutation in the real situation, characterised by a steep voltage drop and a correspondingly abrupt rise in current. This indicates that while a boundary layer is established, its cooling is insufficient. Although after 20 microseconds there is a noticeable cooling effect, the system requires prolonged cooling to prevent re-ignition. This observation is critical to our proposed mitigation strategy, suggesting that extending the cooling duration could effectively address the issue.

B. Mitigation of re-ignition

Based on observations from realistic cases, it has been noted that despite successful current commutation, the residual heat within the boundary layer remains high, around 5000K. This intense heat maintains an ionised channel in the gap, creating a conducive environment for electrical breakdown and the potential for arc re-ignition. In contrast to the voltage profiles of the well-cooled cases as in Figure 4, to prevent arc re-ignition, it is suggested that both the magnitude and slope of the arc voltage should be consistent with the rate of capacitor charging. The intention is to keep zero current through the air gap for longer times to ensure that the gap cools down and the breakdown voltage exceeds the modelled arc fall voltage so the reignition does not take place in practice. Referring to the realistic cooling case voltage profiles in Figure 10, adjustments could include shifting the air gap voltage rightward or increasing the capacitor charging rate. Two methods are proposed to test these strategies effectively: increasing the arc fall voltage and enhancing the capacitor's value.

Strategy 1: Increasing the Arc Fall Voltage

Typically, to enhance the arc fall voltage, one might opt for electrodes composed of specialised material or leverage the voltage-current characteristics of the arc root [22], which exhibit a significant voltage change with current variation.

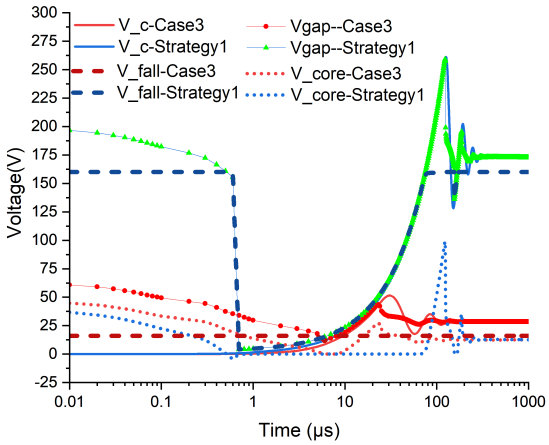

Fig. 12: Comparison of voltage profile across the air gap and capacitor by increasing the arc fall voltage

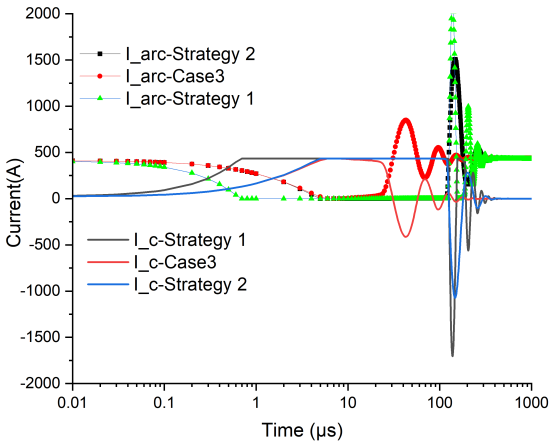

Fig. 13: Comparison of current profile goes through the air gap and capacitor by increasing the arc fall voltage and increasing the capacitor value

By increasing the arc fall voltage, we effectively raise the voltage threshold necessary to sustain the arc. Making the arc fall voltage ten times higher could be a strategy to ensure that the voltage required to maintain the arc is beyond the system operating conditions, allowing more time for the boundary layer to cool down and the arc channel to deionise, thereby reducing the likelihood of arc re-ignition. For circuit behaviours as shown in Figure 12, we could see the voltage profile of the air gap shows a rightward shift than Figure 10 and the same

charging rate as the high cooling rate case. Then we move to the physical phenomena side as demonstrated in Figure 14. As time varies, the cold boundary layer is observed within 1 ms and there is no re-ignition observed. Controlling the system's maximum voltage feasibly involves enhancing electrode heat dissipation, modifying material properties to withstand higher thresholds, and improving the cooling mechanisms of the gap.

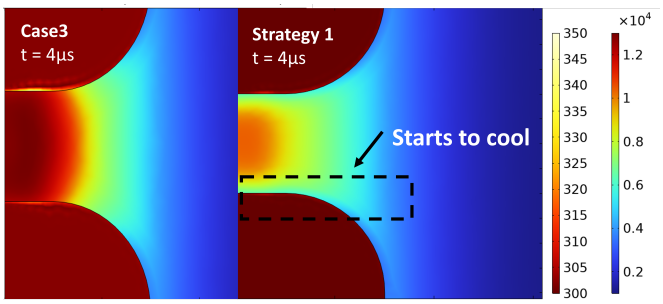

(a) At 4×10^{-6} s

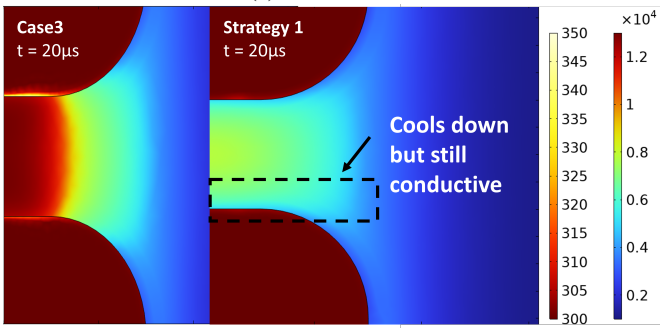

(b) At 2×10^{-5} s

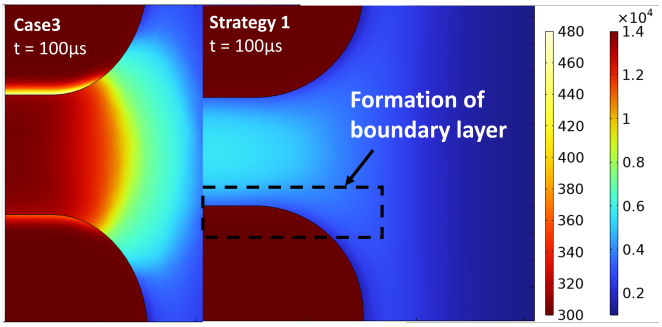

(c) At 1×10^{-4} s

Fig. 14: The demonstration of boundary layer formation as time evolution by increasing the arc fall voltage

Strategy 2: Controlling the Voltage Increase Rate of the Capacitor

If the voltage across the capacitor rises at a rate that matches the increase in the arc voltage, it can help prevent a potential difference that might cause a re-ignition. We implemented a four-times bigger value of capacitor to make it charge more in the same time frame. As we observed in Figure 15, the capacitor charging rate shows the same slope at $t = 3\mu$s. This controlled rise allows the boundary layer to cool and the arc

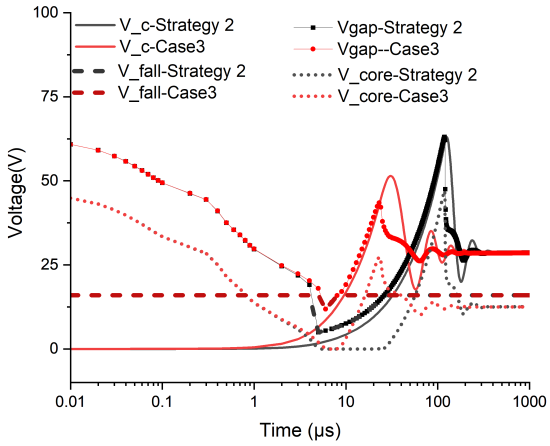

Fig. 15: Comparison of voltage profile across the air gap and capacitor by increasing the capacitor value

to extinguish fully before the voltage can reach a level that would support a re-ignition .

When comparing these two mitigation methods, it is observed that the rate of change in Method 1 is more pronounced than in Method 2, leading to distinct temperature distributions at the initial stage of $t = 0.001$ms. However, as time progresses, both methods allow for the boundary layer to cool down, and the formation of the boundary layer is observed in both strategies, as indicated in the referenced figures for temperature profiles of Method 1 in Figure 14 and Method 2 in Figure 16. For the current behaviours shown in Figure 13, the current still re-strikes with a delay, which is not what we expected in reality. Although we no longer observe an arc, the arc sheath may be breaking through, allowing a low current to still pass through it. Also, the figure 13 illustrates the dangers of re-strike due to energy leakage, where the peak current exceeds the initial interruption current by more than seven times. This is highly dangerous and indicates the need for careful and conservative system development. To avoid the re-ignition phenomena in a DC breaker using a thermal plasma model, managing the temperature of the boundary layer post-commutation is critical. Effective strategies include increasing the arc fall voltage to elevate the breakdown threshold and controlling the voltage increase across the capacitor to allow sufficient cooling time. The clear message is that while these strategies can interrupt the current, choosing the parameters conservatively is essential. Implementing these strategies requires meticulous consideration of the circuit design and the dynamic behaviours of thermal plasma under varying electrical and thermal conditions.

IV. Conclusion

In this paper, we investigate the physical mechanisms responsible for re-ignition phenomena in novel compact circuit breakers. We examined three different cases of arc decay. The

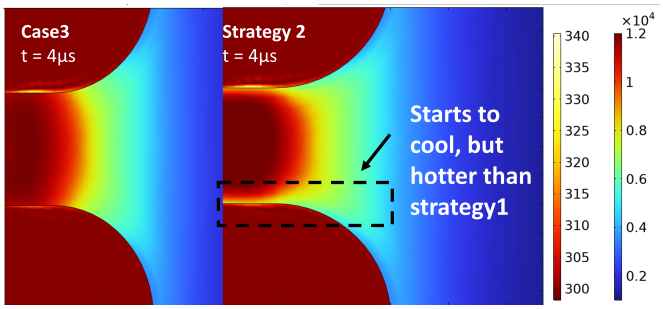

(a) At 4×10^{-6} s

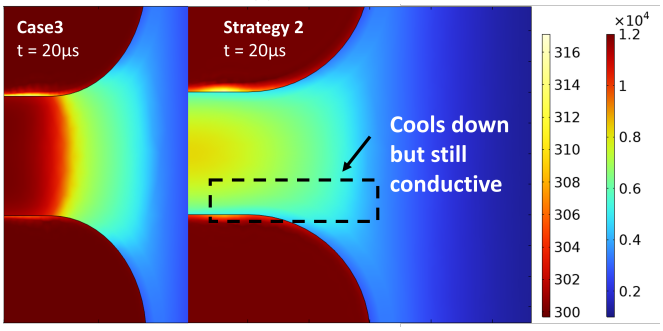

(b) At 2×10^{-5} s

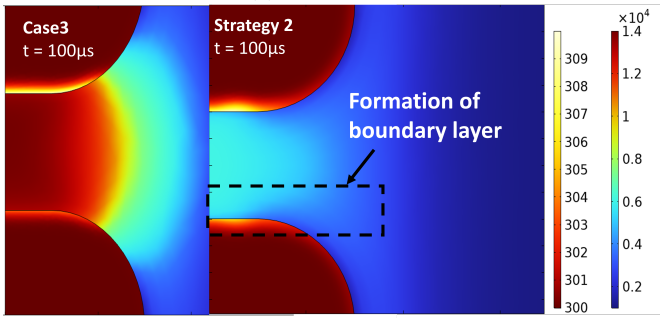

(c) At 1×10^{-4} s

Fig. 16: The demonstration of boundary layer formation as time evolution by increasing the capacitor value

findings reveal that the key to preventing re-ignition lies in the formation of a cool boundary layer. To enhance this formation, two strategies are identified: increasing the arc root voltage, which in turn raises the breakdown threshold of the air gap, or using a larger capacitor to extend the cooling period. This research provides insights for future circuit breaker design. By optimising the cooling efficiency of the boundary layer, it is possible to effectively manage re-ignition, offering the potential to scale up these compact devices for higher current and voltage levels, and unlocking the possibility of adapting these compact devices for future MT HVDC grids.

However, the current model has its limitations. In reality, we observed that electric breakdown occurs in cold air before thermal breakdown. The existing model does not combine electric breakdown with thermal breakdown, which is a significant limitation. Addressing this will be the focus of future work, where we aim to integrate both mechanisms to provide a more comprehensive understanding of the re-ignition process and further improve circuit breaker designs.

REFERENCES

[1] C. M. Franck, "HVDC circuit breakers: A review identifying future research needs," *IEEE transactions on power delivery*, vol. 26, no. 2, pp. 998–1007, 2011.

[2] M. Jansen, C. Duffy, T. C. Green, and I. Staffell, "Island in the sea: The prospects and impacts of an offshore wind power hub in the north sea," *Advances in Applied Energy*, vol. 6, p. 100090, 2022.

[3] M. Guo, X. Li, Z. Gao, and G. Su, "Simulation and analysis on stability improvement of zhangbei renewable energy transmission via VSC-HVDC based on RTDS," in *2020 4th International Conference on HVDC (HVDC)*. IEEE, 2020, pp. 299–303.

[4] R. P. Smeets and N. A. Belda, "High-voltage direct current fault current interruption: A technology review," *High Voltage*, vol. 6, no. 2, pp. 171–192, 2021.

[5] D. Jovcic and B. Wu, "Fast fault current interruption on high-power DC networks," in *IEEE PES General Meeting*. IEEE, 2010, pp. 1–6.

[6] M. Hajian, D. Jovcic, and B. Wu, "Evaluation of semiconductor based methods for fault isolation on high voltage DC grids," *IEEE Transactions on Smart Grid*, vol. 4, no. 2, pp. 1171–1179, 2013.

[7] L. Tang and B.-T. Ooi, "Locating and isolating DC faults in multi-terminal DC systems," *IEEE transactions on power delivery*, vol. 22, no. 3, pp. 1877–1884, 2007.

[8] F. Mohammadi, K. Rouzbehi, M. Hajian, K. Niayesh, G. B. Gharehpetian, H. Saad, M. H. Ali, and V. K. Sood, "HVDC circuit breakers: A comprehensive review," *IEEE Transactions on Power Electronics*, vol. 36, no. 12, pp. 13 726–13 739, 2021.

[9] D. Jovcic, "Fast commutation of DC current into a capacitor using moving contacts," *IEEE Transactions on Power Delivery*, vol. 35, no. 2, pp. 639–646, 2019.

[10] K. Tahata, S. El Oukaili, K. Kamei, D. Yoshida, Y. Kono, R. Yamamoto, and H. Ito, "HVDC circuit breakers for HVDC grid applications," in *11th IET international conference on AC and DC power transmission*. IET, 2015, pp. 1–9.

[11] N. A. Belda, R. P. P. Smeets, and R. M. Nijman, "Experimental investigation of electrical stresses on the main components of HVDC circuit breakers," *IEEE Transactions on Power Delivery*, vol. 35, no. 6, pp. 2762–2771, 2020.

[12] F. Karetta and M. Lindmayer, "Simulation of the gasdynamic and electromagnetic processes in low voltage switching arcs," in *Electrical Contacts-1996. Proceedings of the Forty-Second IEEE Holm Conference on Electrical Contacts. Joint with the 18th International Conference on Electrical Contacts*. IEEE, 1996, pp. 35–44.

[13] G. Lehner, "Elektromagnetische feldtheorie fuer physiker und ingenieure," *Springer Verlag, Berlin, Heidelberg*, vol. 10, pp. 978–3, 1990.

[14] J. Lowke, "Predictions of arc temperature profiles using approximate emission coefficients for radiation losses," *Journal of Quantitative Spectroscopy and Radiative Transfer*, vol. 14, no. 2, pp. 111–122, 1974.

[15] A. B. Murphy, "Transport coefficients of air, argon-air, nitrogen-air, and oxygen-air plasmas," *Plasma chemistry and plasma processing*, vol. 15, pp. 279–307, 1995.

[16] Y. P. Raizer, "Gas discharge physics," 1991.

[17] M. Benilov, "Understanding and modelling plasma–electrode interaction in high-pressure arc discharges: a review," *Journal of Physics D: Applied Physics*, vol. 41, no. 14, p. 144001, 2008.

[18] M. Benilov, L. Benilova, H.-P. Li, and G.-Q. Wu, "Sheath and arc-column voltages in high-pressure arc discharges," *Journal of Physics D: Applied Physics*, vol. 45, no. 35, p. 355201, 2012.

[19] A. Gleizes, J.-J. Gonzalez, and P. Freton, "Thermal plasma modelling," *Journal of Physics D: Applied Physics*, vol. 38, no. 9, p. R153, 2005.

[20] J. Nan, G. Chen, and I. Golosnoy, "Modelling of arcing phenomena during opening contacts in novel circuit breaker," in *Proceedings of the 22nd International Symposium on High Voltage Engineering*. IET, 2023, pp. 701–707.

[21] J. Arrillaga, *High voltage direct current transmission*. IET, 1998, no. 29.

[22] A. Mutzke, T. Rüther, M. Lindmayer, and M. Kurrat, "Arc behavior in low-voltage arc chambers," *The European Physical Journal-Applied Physics*, vol. 49, no. 2, p. 22910, 2010.